

TO: Jim McGregor-Dawson  
CC:  
FROM: David McInnes  
DATE: November 13, 2011  
SUBJECT: Compass Creek IP Modelling - Executive summary

---

The eight IP traverses collected in August/September 2011 over the Compass Creek Project area (figure 1), have been modelled and integrated into a comprehensive 3D model combining: 3D magnetic modelling (ground & airborne data), geochemistry, geology, AEM and structure (figure 2).

From the combined model several areas of interesting are defined. For the northern three traverses the most interesting of these are (in no ranking order):

- A subtle chargeable source with depth extent directly associated with the mapped Kamas Cauldron (figure 3a). The chargeable body correlates with a deepening of the weathering profile (as indicated by the resistivity model) which also has a slight increase in conductive (increased clay/water?). There does not appear to be any geochemical anomaly associated with the chargeable body.
- Beneath the mapped location of the Jason's Peak breccia pipe there is a substantial chargeable body associated with a strong conductor (figure 3b). Also associated with this location are elevated Pb and Ag rock chip assays. The IP traverse directly to the south of the Jason's Peak breccia displays a more diffuse chargeable conductor, indicating that the source may have deepened, however more likely it suggests that the source of the anomaly is off line.
- Directly to the east of the chargeable conductor associated with the Jason's Peak breccia there is another strong chargeable conductor. The body occurs directly below the mapped NNW striking alteration/ quartz vein zone. The depth to the top of this body is deeper than that of the Jason's Peak source, however it still displays an associated elevated rock chip geochemistry above it. The IP traverse directly to the south displays the chargeable conductor as a "diffuse/nebulous" deep feature indicating that the source is off line. Both this chargeable conductor and the one associated with the Jason's Peak breccia are open to the north.

The integrated model in the south of the project area, over the strong "bull's eye" magnetic anomaly, is slightly more complex than that for the three traverses in the north of the project area. The 3D magnetic inversions for both the ground and airborne magnetic data are remarkable similar; with, of course, the ground magnetic data producing more resolution/complexity. The resultant 3D magnetic models produce an anticline structure with moderate magnetic limbs dipping in correlation with the mapped anticline (figure 4). In the hinge of the anticline is a strong magnetic core that plunges to the north (figure 5).

Most of the chargeability encountered in this hinge zone appears to occur above and/or on the flanks of this magnetic core (figure 6). The chargeable modelling indicates that the area above the magnetic fold hinge is a broad depth limited chargeable zone with areas of isolated/discrete elevated chargeability. The depth to these discrete chargeable sources is shallow to nearly outcropping and only low level elevated rock chip geochemistry appears to be recorded above these areas. The Tempest AEM data defined a moderate conductor in

the core of the fold, this correlates with a moderate conductive zone defined in the modelling of the IP resistivity data (figure 7).

For the lines to the north of the fold hinge (8513250n) there are some interesting chargeable bodies that appear to be controlled (trending and terminated) by the structures identified by terra search from their ground magnetic data (figure 8). The chargeable bodies have an interesting spatial association with some conductors and also have some moderately elevated rock chip geochemistry above them.

The stacked model sections for both the northern and southern traverses are presented at the end of this document (figures 9a and 9b). The individual traverse data and model sections are currently in preparation and will be sent through at a later date.

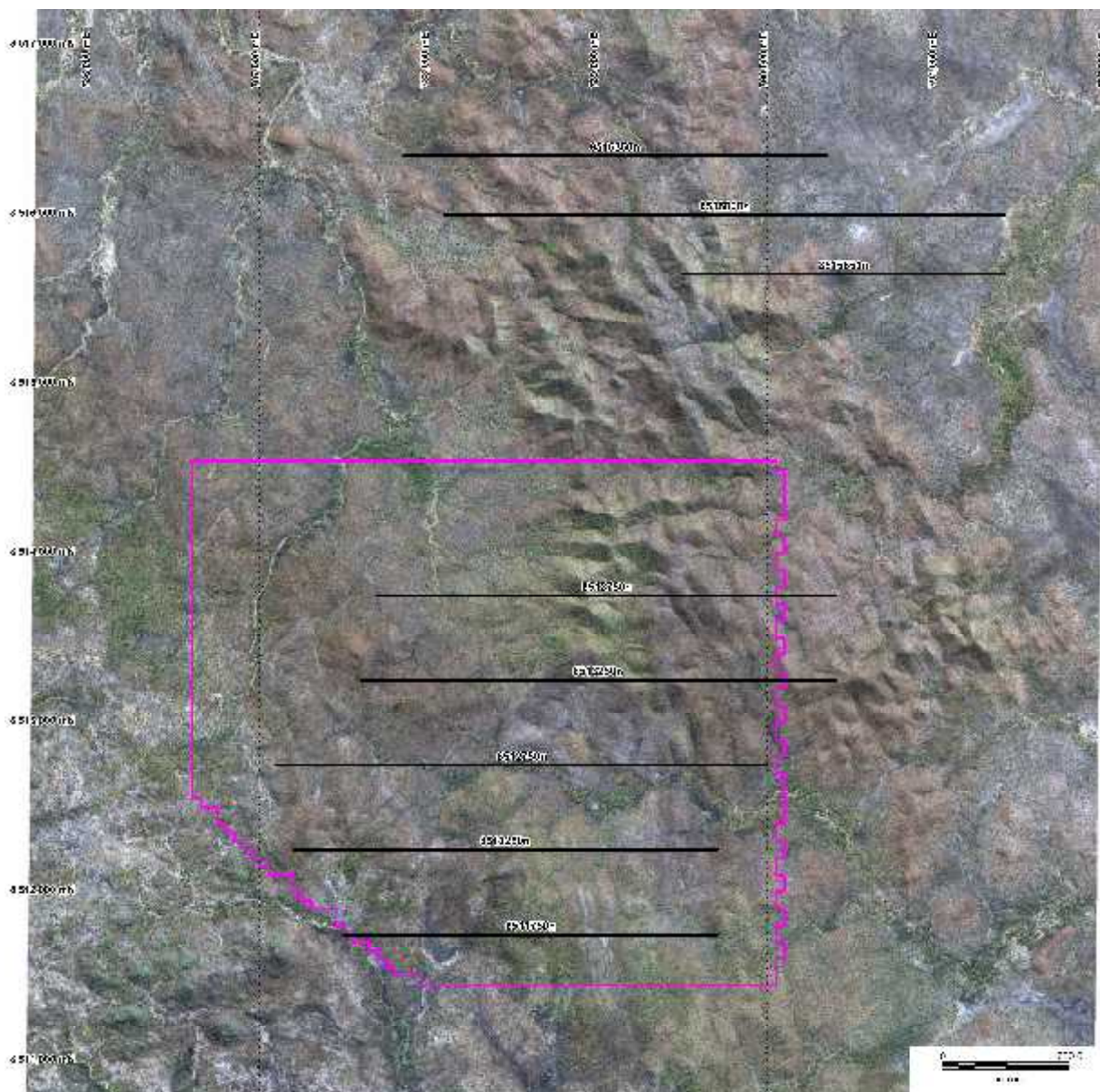


figure 1: location of the IP traverses over the Quickbird image. The magenta [polygon represents the outline of the ground magnetic survey area data (2010).

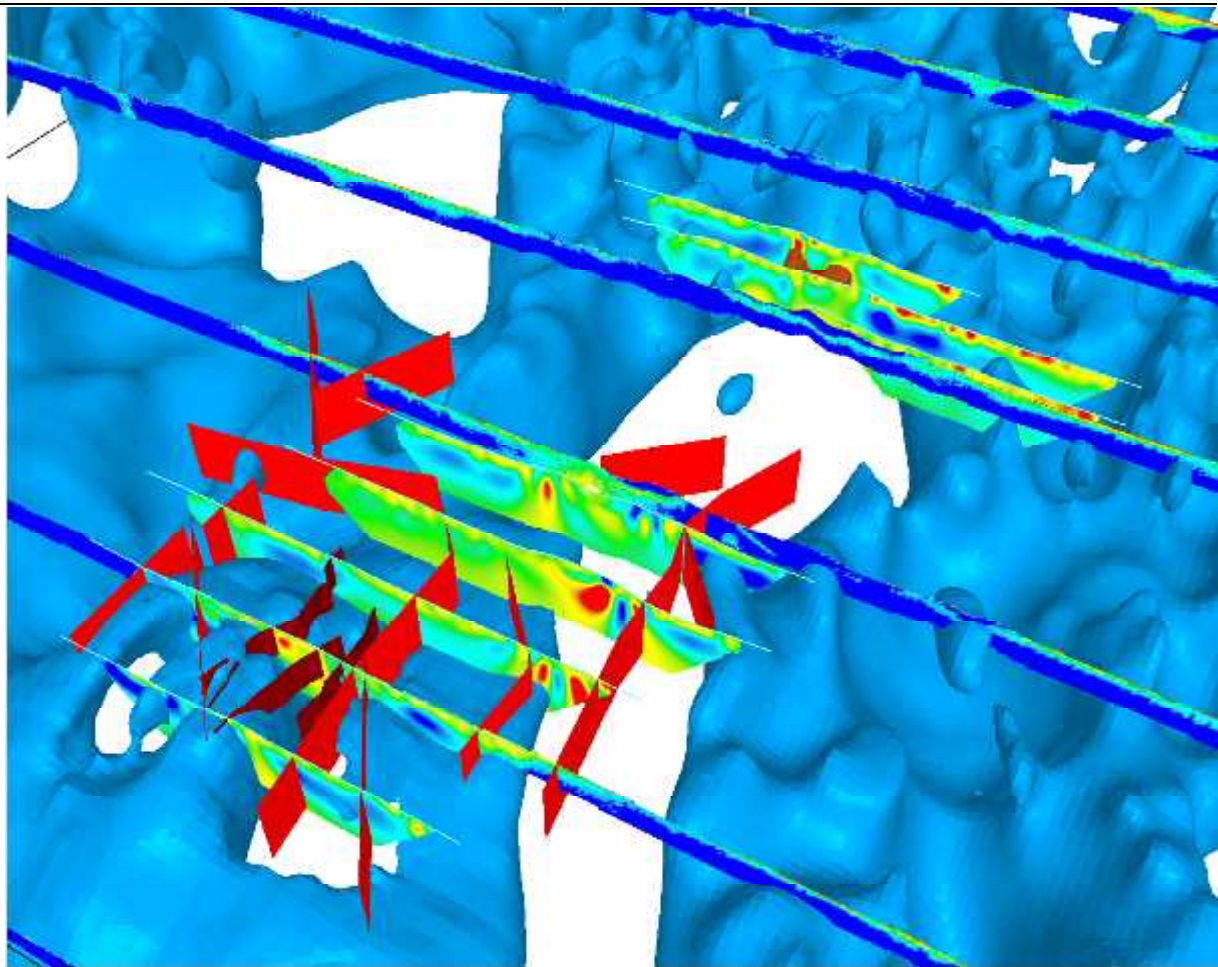


Figure 2: A snap shot of the 3D model displaying the airborne 3D magentic model with the AEM and IP resistivity model sections. Also shown are the Terra-search structures and magnetic trends.

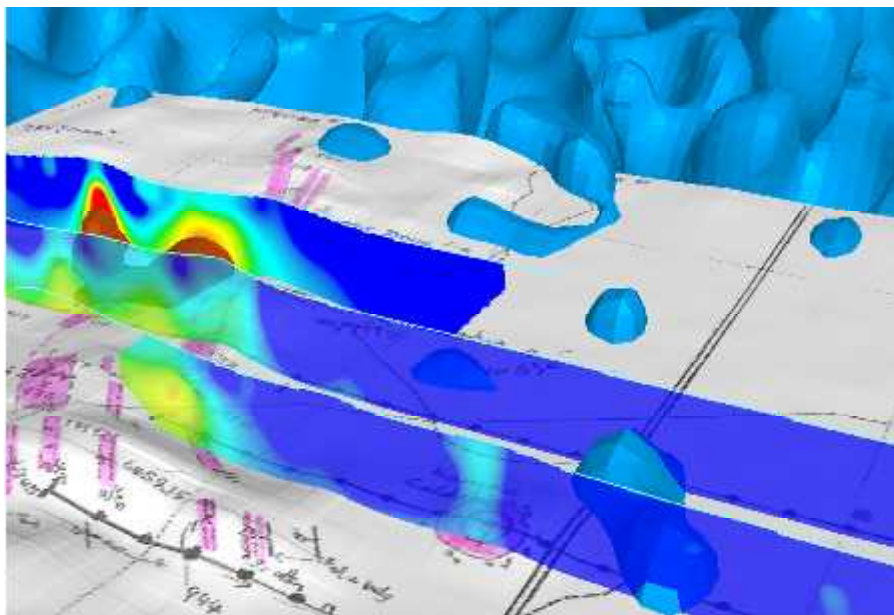


Figure 3a: The Chargeability model section that covers the Kamas Calderon, note the subtle chargeable response associated with its mapped position.

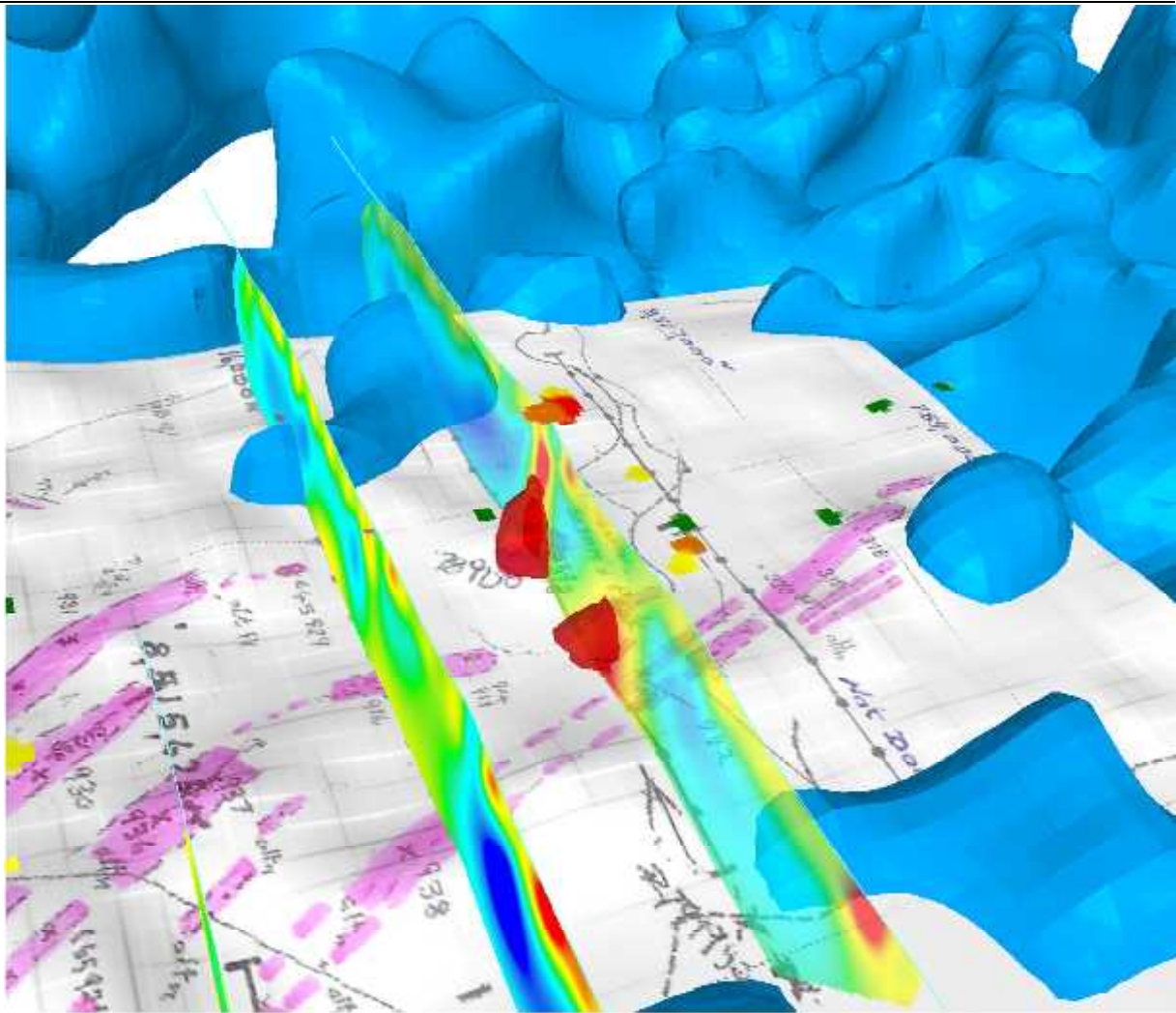


Figure 3b: A snap shot of the 3D model displaying the chargeability shells along with the resistivity model sections, the 3D magnetic model susceptibility shells, the Lead rock chip geochemistry and the alteration/vein mapping (displaced downwards 250m). Note the two strong chargeable bodies that are associated with conductors and elevated geo-chemistry

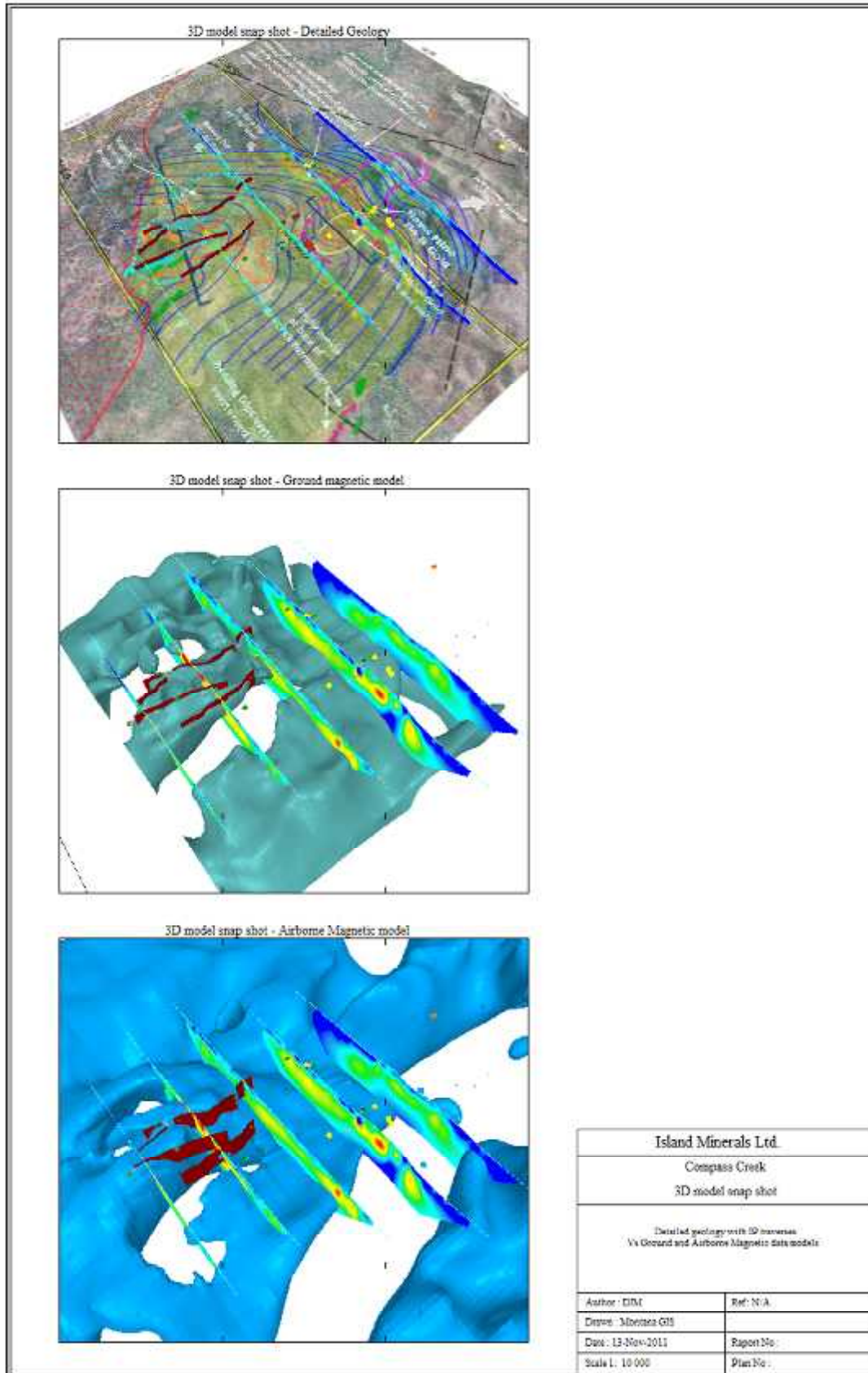


Figure 4: A comparison of the 3D magnetic shells from the ground and airborne magnetic data models with the detailed geology map image at the top.

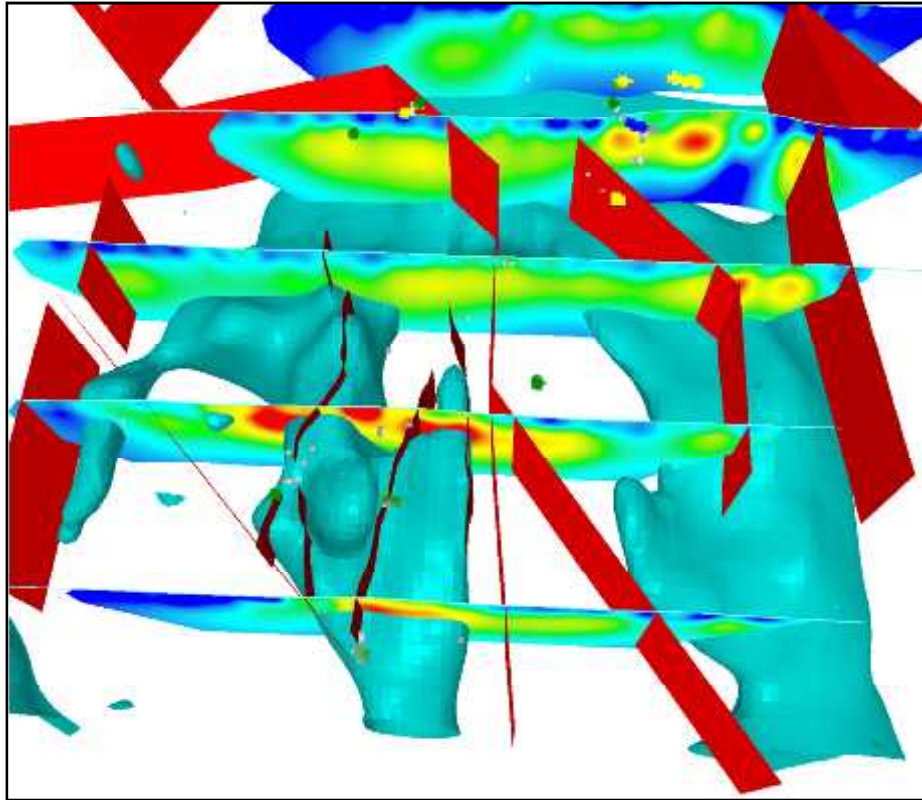


Figure 5: A snap shot of the 3D model with the chargeability model sections, the Terra-search structures and the magnetic susceptibility shells. Note how the core of the magnetic anomaly plunges to the north.

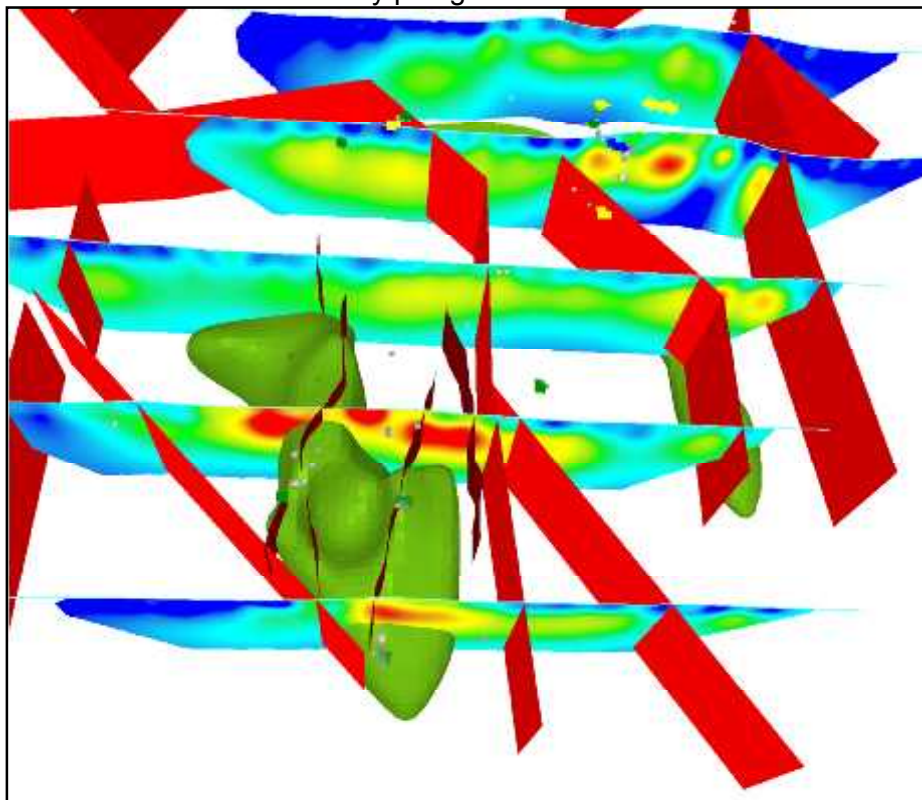


Figure 6: A snap shot of the 3D model with the chargeability model sections, the Terra-search structures and the magnetic susceptibility shells. Note how for the southern traverses associated with the magnetic hinge/core the chargeability sources all sit very shallow above and/or adjacent to the source of the magnetic anomaly.

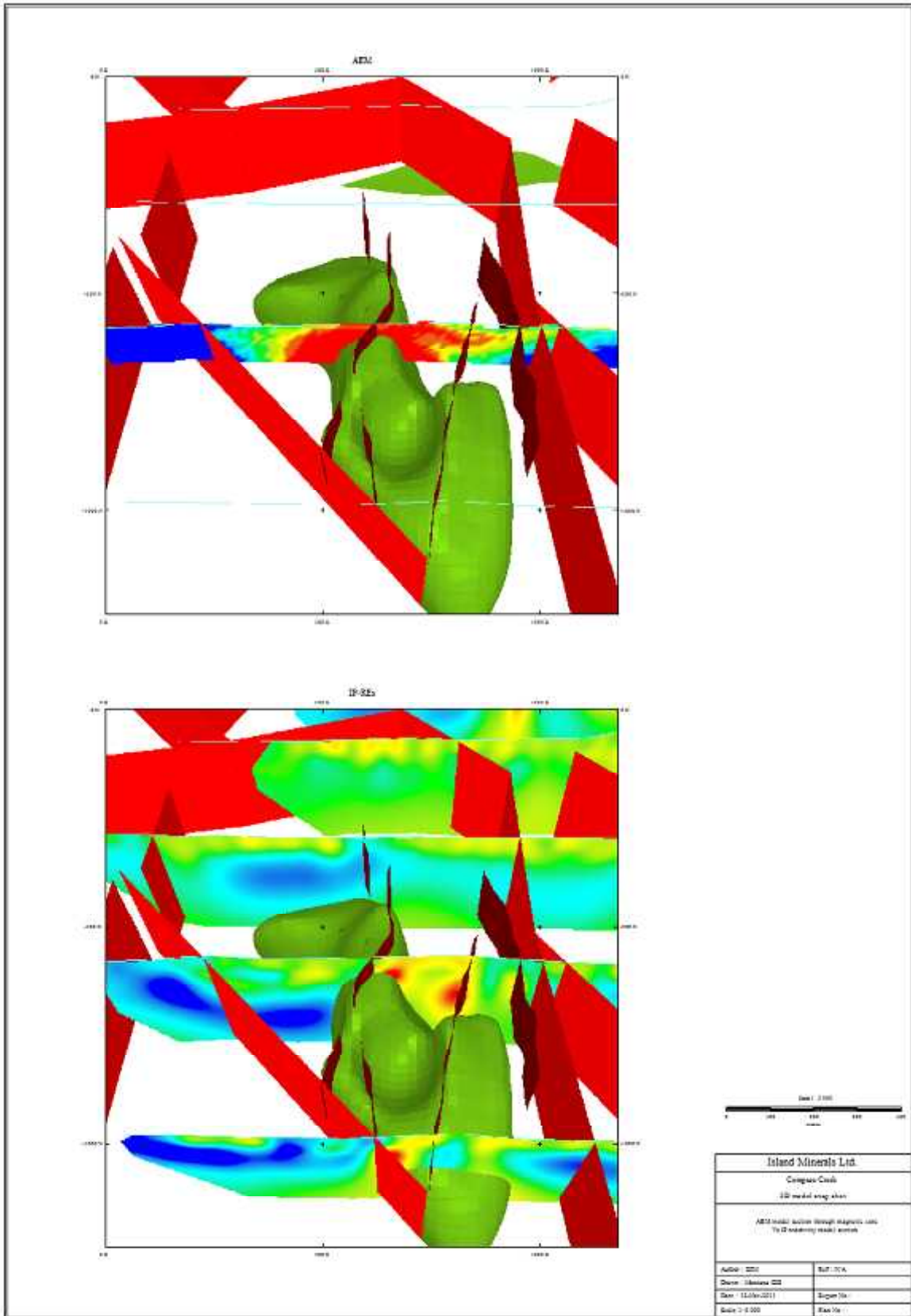


Figure 7: A comparison of the resistivity model section from the AEM data and that from the IP traverses. Also shown are the terra-search ground magnetic structures and trends and the high level susceptibility magnetic shell (green)

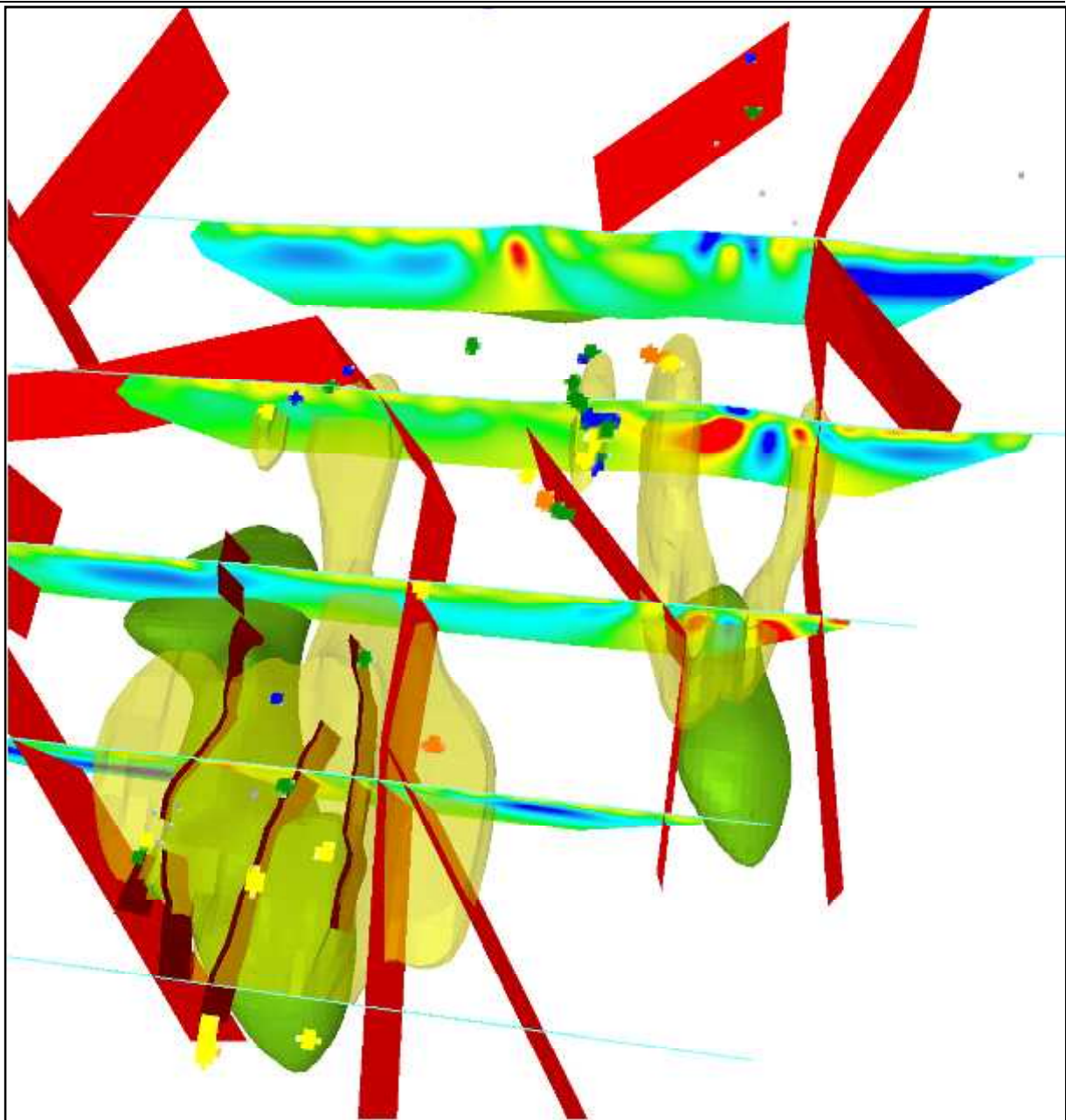


Figure 8: A snap shot of the 3D model displaying a chargeability shell (transparent golden hue) with the IP resistivity model sections, the high susceptibility magnetic shells (green) and the structures defined by terra-search from their ground magnetic data (red). Note how the chargeability shells for the second and third most northern traverse appear to truncated in the south by the structure and how the most western chargeable body correlates directly with the structure.

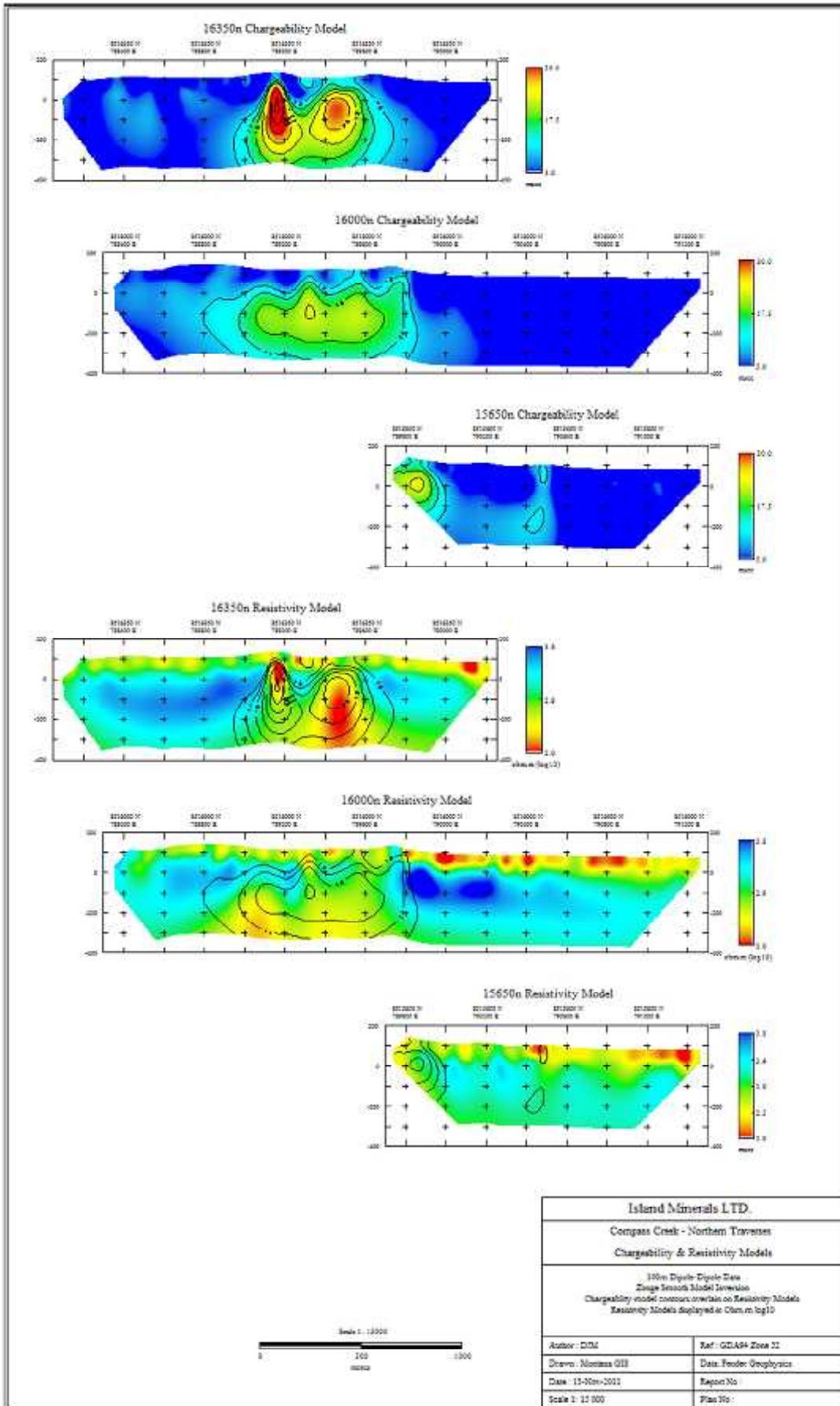


Figure 9a: Stacked model sections for the 3 northern traverses.

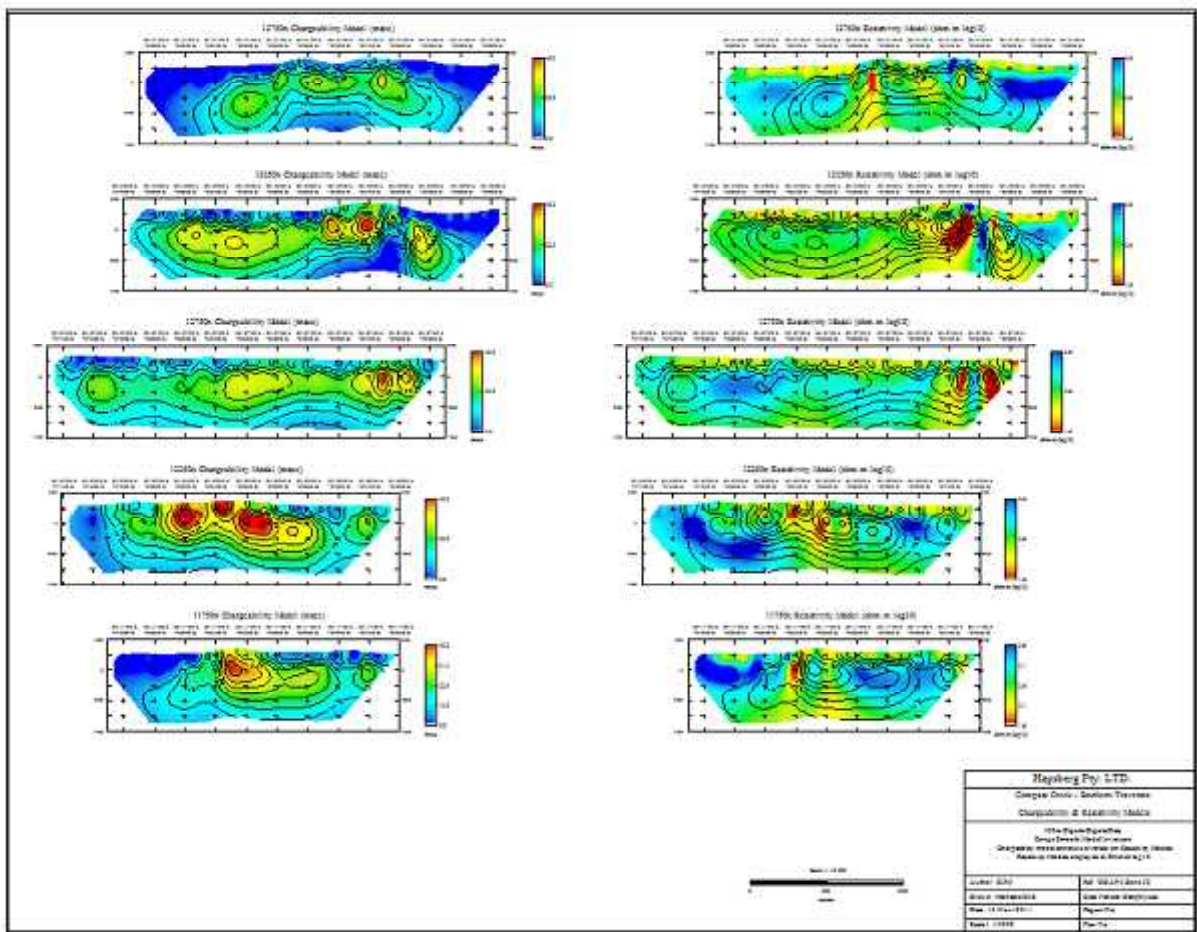


Figure 9b: Stacked model sections for the 5 southern traverses.